Communication

THE JOURNAL OF BIOLOGICAL CHEMISTRY
Vol. 273, No. 19, Issue of May 8, pp. 11413–11416, 1998

Structure of Peptide Deformylase and Identification of the Substrate Binding Site*

(Received for publication, January 12, 1998)

Andreas Becker‡, Ilme Schlichting§, Wolfgang Kabsch‡¶,Sabine Schultz‖, and A. F. Volker Wagner‖

From the ‡Max-Planck-Institut für medizinische Forschung, Abteilung Biophysik, Jahnstrasse 29, 69120 Heidelberg, Germany, §Max-Planck-Institut für molekulare Physiologie, Abteilung Physikalische Biochemie, Rheinlanddamm 201, 44139 Dortmund, Germany, and ‖Biochemie-Zentrum Heidelberg, Ruprecht-Karls Universität, Im Neuenheimer Feld 501, 69120 Heidelberg, Germany

Peptide deformylase is an essential metalloenzyme required for the removal of the formyl group at the N terminus of nascent polypeptide chains in eubacteria. The *Escherichia coli* enzyme uses Fe^{2+} and nearly retains its activity on substitution of the metal ion by Ni^{2+}. We have solved the structure of the Ni^{2+} enzyme at 1.9-Å resolution by x-ray crystallography. Each of the three monomers in the asymmetric unit contains one Ni^{2+} ion and, in close proximity, one molecule of polyethylene glycol. Polyethylene glycol is shown to be a competitive inhibitor with a K_I value of 6 mM with respect to formylmethionine under conditions similar to those used for crystallization. We have also solved the structure of the inhibitor-free enzyme at 2.5-Å resolution. The two structures are identical within the estimated errors of the models. The hydrogen bond network stabilizing the active site involves nearly all conserved amino acid residues and well defined water molecules, one of which ligates to the tetrahedrally coordinated Ni^{2+} ion.

In eubacteria as well as in mitochondria and chloroplasts the amino group of methionyl-$tRNA_f^{Met}$ is *N*-formylated by a formyltransferase during initiation of protein synthesis (1). Consequently, all nascent polypeptides are synthesized with *N*-formylmethionine at the N terminus. During elongation of the polypeptide chain the formyl group is removed hydrolytically by the enzyme peptide deformylase (PDF,[1] EC 3.5.1.27) (2, 3). For *Escherichia coli*, deletion of the formyltransferase gene leads to a strongly reduced cell growth rate (4), whereas deletion of the PDF gene proves lethal (5). This formylation/deformylation cycle, which appears to be a characteristic feature of eubacteria, does not occur in the cytoplasm of eucaryotic cells. Therefore, PDF is an attractive target for the design of new antibiotics.

PDF from *E. coli*, a monomeric protein of 168 residues, shares the fingerprint motifs H*EXX*H (6), EGCLS, and G*X*G*X*-AA*X*Q (7) with PDF sequences of other eubacteria, which suggests a common architecture of the catalytic region in these proteins. PDF was reported to be a zinc enzyme (8) that contains the motif H*EXX*H, known to be involved in zinc binding in metalloproteases (9, 10). Meanwhile, it has been shown that PDF utilizes Fe^{2+} as catalytic metal whereas the Zn^{2+} form is nearly inactive (11, 12). Interestingly, Fe^{2+} can be replaced by Ni^{2+} with a slight reduction in PDF activity (11).

Recently, the structure of the core domain (residues 1–147) of PDF was solved by NMR (8) and the structure of the full-length protein by x-ray crystallography at 2.9-Å resolution (13). Both structures describe the protein as isolated with a tightly bound zinc ion. We report the structure of the catalytically active enzyme in the nickel-bound form (PDF-Ni) at 2.5-Å resolution and at 1.9-Å resolution in complex with a polyethylene glycol molecule (PDF-Ni/PEG), shown here to be a competitive inhibitor of the enzyme.

EXPERIMENTAL PROCEDURES

PDF-Ni (specific activity, 900 units/mg; 0.6 Ni^{2+} ions per protein molecule) was isolated from overproducing *E. coli* cells and crystallized with 2 M $(NH_4)_2SO_4$ as precipitant in the presence of 1% (w/v) PEG-1000 as described.[2] Crystals were washed in 100 mM MOPS/NH_3, 1% (w/v) PEG-1000, 2 M $(NH_4)_2SO_4$ at pH 7.4. Three isomorphous derivatives were obtained by soaking crystals in the above buffer with added heavy atom compounds. The mercury derivative crystals were harvested after soaking 12 h in 0.1 mM ethylmercury phosphate (EMP), the platinum derivative after soaking 24 h in 2 mM K_2PtCl_4, and the double derivative after soaking 24 h in 0.1 mM CH_3HgCl and 2 mM K_2PtCl_4. PDF-Ni crystals without PEG have been described.[2]

Diffraction data were collected at room temperature by the rotation method and recorded by an electronic area detector (x-rays: CuK_α, focused by Franks double-mirror optics; generator: GX-18, Elliot/Enraf-Nonius, Delft, operated at 35 kV/50 mA; detector: X100, Siemens/Nicolet, Madison, WI; crystal to detector distance: 10 cm; rotation/image: 0.0417° or 0.0833°). Integrated intensities were extracted from the rotation images by the program XDS (15), which includes routines for space group determination from the observed diffraction pattern (16).

Inhibition of PDF by PEG-1000 was determined by the following procedure. PDF activity was measured at 30 °C with formyl-Met (1–32 mM) at pH 7.2 (100 mM MOPS/NaOH, 2 M Li_2SO_4, 1 mM TCEP) in a total volume of 50 μl. The reaction was started by 420 ng of PDF-Ni (5 μl) and stopped after 5 min by 4% $HClO_4$ (50 μl). The amount of hydrolyzed substrate was determined according to the method of Fields (17) using 2,4,6-trinitrobenzolsulfonic acid (ϵ_{420} = 22 mM^{-1} cm^{-1}). For inhibition studies, up to 10 mM PEG-1000, pretreated with TCEP (350 mM PEG/35 mM TCEP, pH 7.2) for 1 h, was included in the assay mixture. V_{max} and apparent K_M values were estimated from double-reciprocal plots (1/*v* *versus* 1/[S]), and the K_I value was calculated from secondary replots of the slopes *versus* PEG-1000 concentrations.

RESULTS

Structure Determination—Crystallographic data used for structure determination are summarized in Table I. The structure of PDF-Ni/PEG crystals was solved by the multiple isomorphous replacement method and exploitation of the 3-fold redundancy of the electron density in the asymmetric unit. The atomic model was obtained by several rounds of model building

* The costs of publication of this article were defrayed in part by the payment of page charges. This article must therefore be hereby marked "*advertisement*" in accordance with 18 U.S.C. Section 1734 solely to indicate this fact.

The atomic coordinates (entry code 1ICJ) and structure factors (entry code R11CJSF) have been deposited in the Protein Data Bank, Brookhaven National Laboratory, Upton, NY.

¶ To whom correspondence should be addressed. Tel.: 6221-486-276; Fax: 6221-486-437; E-mail: kabsch@mpimf-heidelberg.mpg.de.

[1] The abbreviations used are: PDF, peptide deformylase; PEG, polyethylene glycol; MOPS, 3-morpholinopropanesulfonic acid; TCEP, tris(2-carboxyethyl)phosphine; r.m.s., root mean square.

[2] Groche, D., Becker, A., Schlichting, I., Kabsch, W., Schultz, S., and Wagner, A. F. V. (1998) *Biochem. Biophys. Res. Commun.*, in press.

TABLE I
Statistics of crystallographic data

PDF-Ni/PEG Resolution bins (Å)	Space group *C2*, a = 140.7 Å, b = 63.4 Å, c = 86.9 Å, β = 120.6°					
	Overall	∞–6.0	6.0–4.0	4.0–3.0	3.0–2.0	2.0–1.9
Native						
R_{sym} (%)[a] (6 crystals)	7.5	5.5	5.9	7.2	13.6	24.7
Mean redundancy[b]	5.5	11.7	9.5	8.8	4.6	2.1
Completeness (%)	97.9	98.1	99.5	99.7	97.9	95.3
$\langle I/\sigma \rangle$	21.8	85.7	70.6	43.6	10.8	2.7
R (%)[c]	20.6		15.8	16.9	23.3	31.2
R_{free} (%)[d]	24.0		21.1	20.2	26.2	32.4
Mean figure of merit	0.60	0.81	0.67	0.52		
EMP						
Completeness (%)	85.6	87.0	91.2	82.4		
Phasing power[e]	2.1	3.3	2.0	1.3		
R_C (%)[f]	43.4	28.7	44.4	57.1		
K_2PtCl_4						
Completeness (%)	97.4	97.3	99.3	96.4		
Phasing power[e]	2.0	3.6	1.7	1.2		
R_C (%)[f]	45.2	26.2	48.7	62.6		
CH_3HgCl/K_2PtCl_4						
Completeness (%)	98.6	94.9	98.9	99.2		
Phasing power[e]	1.5	2.2	1.4	1.1		
R_C (%)[f]	56.2	40.0	59.5	68.9		

PDF-Ni Resolution bins (Å)	Space group *C2*, a = 143.4 Å, b = 64.0 Å, c = 84.5 Å, β = 123.0°					
	Overall	∞–6.0	6.0–4.0	4.0–3.0	3.0–2.6	2.6–2.5
Native						
R_{sym} (%)[a] (5 crystals)	8.6	5.9	6.1	9.5	22.6	33.3
Mean redundancy[b]	4.1	4.4	4.5	4.3	3.8	3.6
Completeness (%)	97.2	98.5	99.4	98.4	95.5	94.3
$\langle I/\sigma \rangle$	17.4	48.4	35.4	16.5	5.0	3.1
R (%)[c]	22.5		18.4	21.2	28.7	32.7
R_{free} (%)[d]	26.9		22.2	25.8	32.9	37.8

[a] $R_{sym} = \Sigma_h \Sigma_i |I_{hi} - I_h| / \Sigma_{hi} I_{hi}$, where h are unique reflection indices and I_{hi} are the intensities of symmetry equivalent reflections giving a mean value of I_h.
[b] Multiplicity of measurements of each unique reflection.
[c] $R = \Sigma |F_{obs} - F_{model}| / \Sigma F_{obs}$, where F_{obs} and F_{model} are observed and atomic model structure factor amplitudes, respectively. Reflections at a lower resolution than 6 Å are excluded from the summation.
[d] R factor calculated for 10% of randomly chosen reflections, which were excluded from the refinement.
[e] Phasing power is the mean value of the heavy atom structure factor amplitude divided by the residual lack-of-closure error.
[f] Cullis R factor for centric reflections.

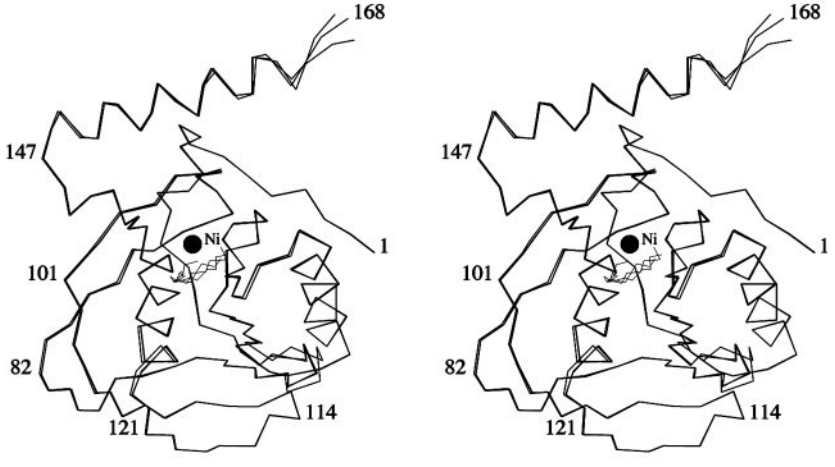

FIG. 1. **Stereo view of superimposed C-α traces of the three crystallographically independent copies of peptide deformylase.** The numbers refer to amino acid residues. The transformations for optimal superposition were determined from equivalent C-α atoms using molecule A as a reference and applied to the Ni^{2+} ion (marked as *Ni*) and the PEG molecule as well.

(18) and correction followed by refinement (19) and map calculation. Atomic coordinates for about 50% of the residues were restrained to obey non-crystallographic symmetry. Unexpected density near the metal ion occurred in all three independent monomers and improved to a clear feature during the refinement process. It was then assumed to be an ordered part of a PEG molecule, consistent with subsequent biochemical studies showing that PEG is a competitive inhibitor of PDF. Only parts of the PEG-1000 molecules ($HO(C_2H_4O)_nH$, $\bar{n}$ = 22) are found in the map at a density above 5% of the map maximum. The visible part is modeled with n = 10 for the molecule length. The final model consists of 4122 (3 × 1346 + 84 alternate locations) non-hydrogen protein atoms, 3 Ni^{2+} ions, 2 SO_4^{2-} ions, 3 PEG, and 205 water molecules. The estimated coordinate error is 0.21 Å, and r.m.s. deviations from ideal geometry are 0.01 Å and 1.2° for bond length and bond angles, respectively.

Structure determination of PDF-Ni crystals was based on the above atomic model. The refined structure consists of 4038 (3 × 1346) non-hydrogen protein atoms, 3 Ni^{2+} ions, 2 SO_4^{2-} ions, and 100 water molecules. The estimated coordinate error is 0.30 Å, and r.m.s. deviations from ideal geometry are 0.015 Å and 1.4° for bond length and bond angles, respectively. In both structures, coordinates for residues Arg-167 and Ala-168 are ill defined, and Pro-9 is found in a *cis*-conformation.

Overall Structure—Basically confirming the results of Chan *et al.* (13), PDF-Ni is an $\alpha + \beta$ protein consisting of a five-stranded antiparallel β-sheet (β_1, β_2, β_3, β_6, β_7), a two-stranded β-ribbon (β_4, β_5), three regular α-helices, and three short 3_{10} helices (Figs. 1 and 2). It has been noticed (8) that this overall arrangement of secondary and tertiary structure is quite different from other metalloproteases such as thermolysin (20) or stromelysin-1 (21), which also contain parallel β-strands.

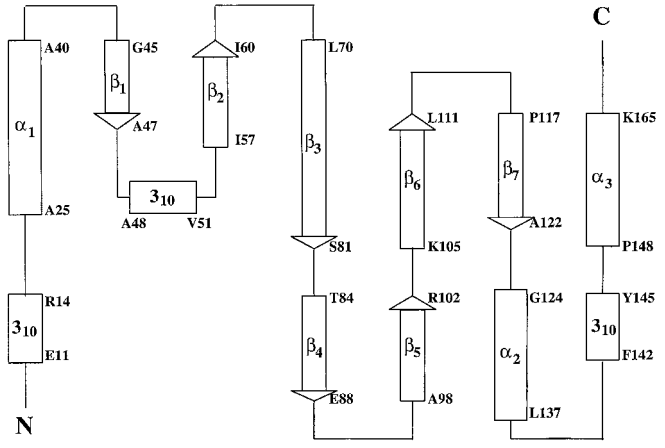

FIG. 2. **Schematic representation of secondary structure as analyzed by the program DSSP (14).** First and last amino acid residues in the helices and sheet strands are specified.

The structures of the three molecules in the asymmetric unit are rather similar except for the more flexible regions 62–68 and 164–168 (Fig. 1). Moreover, a comparison of the monomer structures with and without bound PEG shows no significant differences. In fact, the r.m.s. deviation between corresponding C_α atoms is 0.25 Å (residues 66–68 and 161–168 are omitted from the comparison), which is within the expected coordinate errors of the models. The monomer structure is apparently rigid and structurally insensitive to the binding of PEG and to different environments in the crystal.

Active Site—Sequence alignment of deformylases from other eubacteria reveals three conserved regions, $G^{43}XGXAAXQ$, $E^{88}GCLS$ (7), and $H^{132}EXXH$, which are believed to form the catalytic site of the enzyme involved in metal and substrate binding. Our electron density map at 1.9-Å resolution allows an unambiguous assignment of all non-hydrogen atoms forming the active site (Fig. 3). As reported for the zinc structures (8, 13), the Ni^{2+} ion is found to be tetrahedrally ligated (for review of metal liganding see Ref. 22) to the N-ϵ2 atoms of His-132 and His-136 in the HE*XX*H motif, to the S-γ atom of Cys-90, and to an oxygen atom of the group W1 modeled as a water molecule (Figs. 4 and 5). All four ligands are precisely aligned by an

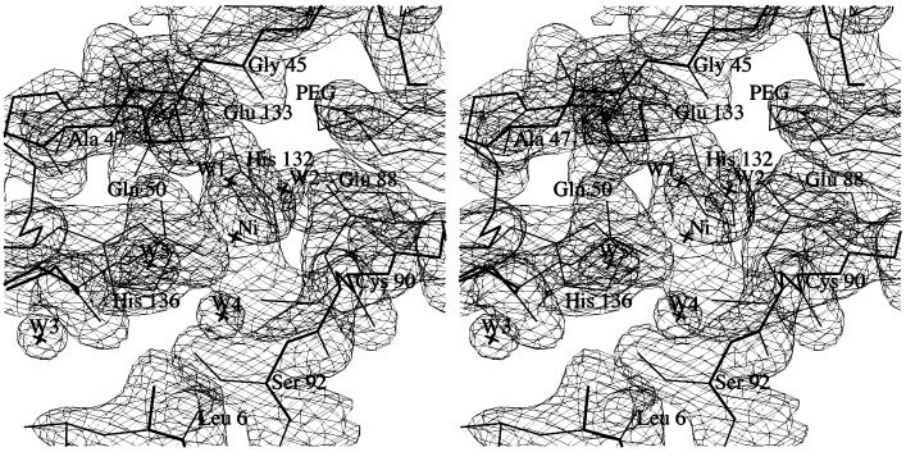

FIG. 3. **Stereo pair of the final σ_A-weighted $2F_o - F_c$ map at 1.9-Å resolution covering the active site of peptide deformylase with the bound Ni^{2+} ion and the ordered part of a PEG molecule.** Density is contoured at 12% of the map maximum.

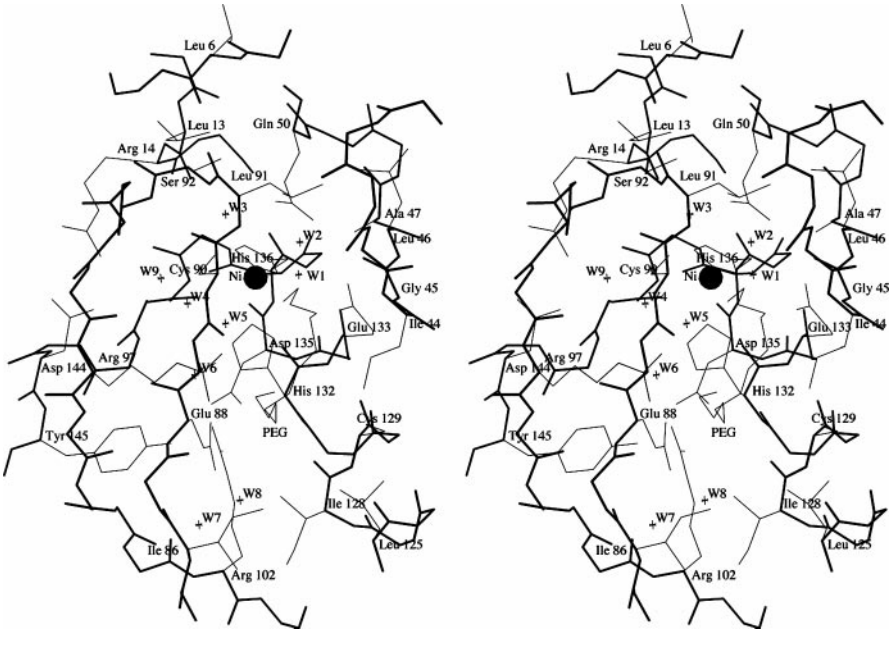

FIG. 4. **Stereo pair of the active site of peptide deformylase showing all non-hydrogen atoms.** Side chain atoms of unlabeled amino acids have been omitted.

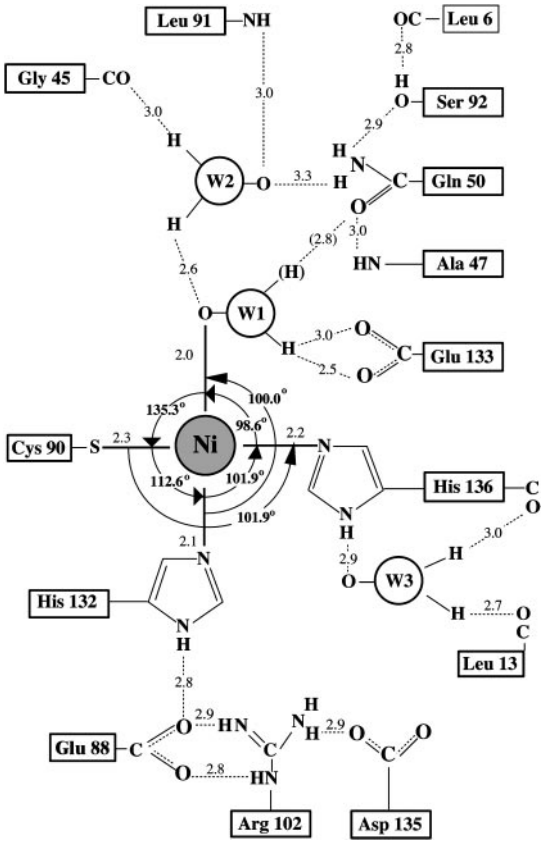

FIG. 5. **Interaction scheme between the catalytic Ni^{2+} ion, water molecules W1, W2, W3, and amino acid residues in the active site of peptide deformylase.** With the exception of Leu-6, all residues shown in the figure are well conserved. Bonds and bond angles between the Ni^{2+} ion and its ligands are shown. *Dashed lines* indicate hydrogen bonds with distances between donor and acceptor atom given in Å. The second proton of W1 and the distance to the side chain of Gln-50 are in brackets to indicate the absence of a hydrogen bond.

intricate network of hydrogen bonds involving conserved residues of the enzyme family. The side chain of His-132 forms a hydrogen bond with the side chain of Glu-88, which itself is fixed by Arg-102 and indirectly by Asp-135. His-136 is held in place by Leu-13 mediated by a water molecule W3. The fourth ligand W1 is fixed by hydrogen bonds with the side chain oxygens of Glu-133 and a water molecule W2. The side chain of Gln-50, although it comes close to W1, is oriented in such a way that it cannot form a reasonable hydrogen bond with W1. In fact, there is no accepting group for the second proton of W1 in our structure, which leads us to speculate that it could well be a hydroxyl anion instead of a water molecule. The side chain of the conserved Gln-50 forms hydrogen bonds donating protons to water W2 and to the hydroxyl group of Ser-92. Interestingly, water W2, the side chain amide of Gln-50, and the main chain amide of Leu-91 are found in the arrangement required for the tetrahedral transition state, if W2 were replaced by the carbonyl oxygen of the formyl group. The amides of Gln-50 and Leu-91 could well serve as an anion trap to compensate the negative charge developing at the formyl oxygen.

The PEG molecule fits into a pocket formed by residues Gly-43, Ile-44, Ile-86, Glu-88–Leu-91, side chain of Arg-97, Cys-129, His-132, Glu-133, and the Ni^{2+} ion. The interactions are predominantly hydrophobic except for the non-conserved Arg-97, which forms a hydrogen bond with the PEG molecule. The close proximity of the PEG molecule to the Ni^{2+} ion and to the conserved residues suggests that it might overlap with the enzyme's substrate/product binding site. For clarification, inhibition studies were carried out as specified under "Experimental Procedures." For PEG-1000 concentrations up to 10 mM, identical k_{cat} values of $4.7 \pm 0.2\ s^{-1}$ were found, whereas the apparent K_M values increased linearly from 4.1 mM (without PEG-1000) to 12.5 mM (with 10 mM PEG-1000), yielding a calculated K_I value of 6 mM. The observed pattern shows that inhibition by PEG-1000 is competitive with respect to formyl-Met.

DISCUSSION

Since its discovery about 30 years ago PDF is known to rapidly lose its activity, which makes its purification difficult (2, 23). Even in recent work with the recombinant enzyme, specific activities have been reported that are off by orders of magnitude (6, 24). Meanwhile, it has been shown that PDF is a Fe^{2+} enzyme (11, 12) instead of a zinc metalloprotease as previously believed (8). Whereas the Zn^{2+} form is nearly inactive (11, 12), we routinely observe 1200 units/mg specific activity for PDF-Fe^{2+} and 900 units/mg for PDF-Ni^{2+} (11).

The three structures now known appear to be generally similar although significant differences remain that could well be of importance for understanding the enzyme mechanism. The two zinc structures (8, 13) have been compared previously (13), and the following discussion focuses on the differences between the zinc and nickel structures determined by x-ray analysis. These differences include Pro-9, which is in a *cis*-conformation as well as two of the three 3_{10} helices, Glu-11–Arg-14 and Phe-142–Tyr-145, which have been modeled as α-helices α_1 and α_4 in the zinc structure (13). Other structural differences are found in the region Glu-87–Leu-99, which includes the β-ribbon. In the active site region the fourth metal ligand corresponding to W1 seems to be displaced, and the important water molecule W2 appears to be absent from the zinc structure. Also, the side chain of Gln-50 is more involved in stabilizing W2 rather than W1, and the amide hydrogens of Leu-91 and Ala-47 are found at distances 5 and 4.6 Å from W1, respectively, which is too far for a hydrogen bond as reported previously (13).

Acknowledgments—We thank Karin Fritz-Wolf, Arnon Lavie, and Klaus Scheffzek for critical discussions and help at various stages of the project, Hans Wagner for excellent maintenance of the x-ray facilities at the MPI Heidelberg, and Ken Holmes and Joachim Knappe for continuous support.

REFERENCES

1. Kozak, M. (1983) *Microbiol. Rev.* **47,** 1–45
2. Adams, J. M. (1968) *J. Mol. Biol.* **33,** 571–589
3. Ball, L. A., and Kaesberg, P. (1973) *J. Mol. Biol.* **79,** 531–537
4. Guillon, J.-M., Mechulam, Y., Schmitter, J.-M., Blanquet, S., and Fayat, G. (1992) *J. Bacteriol.* **174,** 4294–4301
5. Mazel, D., Pochet, S., and Marlière, P. (1994) *EMBO J.* **13,** 914–923
6. Meinnel, T., and Blanquet, S. (1993) *J. Bacteriol.* **175,** 7737–7740
7. Meinnel, T., Lazennec, C., Villoing, S., and Blanquet, S. (1997) *J. Mol. Biol.* **267,** 749–761
8. Meinnel, T., Blanquet, S., and Dardel, F. (1996) *J. Mol. Biol.* **262,** 375–386
9. Vallee, B. L., and Auld, D. S. (1990) *Biochemistry* **29,** 5647–5659
10. Jongeneel, C. V., Bouvier, J., and Bairoch, A. (1989) *FEBS Lett.* **242,** 211 -214
11. Groche, D. (1995) *Characterization of the Iron Center and the Catalytic Mechanism of Peptide Deformylase from Escherichia coli.* Doctoral dissertation, Universität Heidelberg
12. Rajagopalan, P. T. R., Yu, X. C., and Pei, D. (1997) *J. Am. Chem. Soc.* **119,** 12418–12419
13. Chan, M. K., Gong, W., Rajagopalan, P. T. R., Hao, B., Tsai, C. M., and Pei, D. (1997) *Biochemistry* **36,** 13904–13909
14. Kabsch, W., and Sander, C. (1983) *Biopolymers* **22,** 2577–2637
15. Kabsch, W. (1988) *J. Appl. Crystallogr.* **21,** 916–924
16. Kabsch, W. (1993) *J. Appl. Crystallogr.* **26,** 795–800
17. Fields, R. (1972) *Methods Enzymol.* **25,** 464–468
18. Jones, T. A., Zou, J. Y., Cowan, S. W., and Kjeldgaard, M. (1991) *Acta Crystallogr. A* **47,** 110–119
19. Brünger, A. T. (1988) *J. Mol. Biol.* **203,** 803–816
20. Holmes, M. A., and Matthews, B. W. (1982) *J. Mol. Biol.* **160,** 623–629
21. Gooley, P. R., O'Connell, J. F., Marcy, A. I., Cuca, G. C., Salowe, S. P., Bush, B. L., Hermes, J. D., Esser, C. K., Hagmann, W. K., Springer, J. P., and Johnson, B. A. (1994) *Nat. Struct. Biol.* **1,** 111–118
22. Glusker, J. P. (1991) *Adv. Protein Chem.* **42,** 1–76
23. Livingston, D. M., and Leder, P. (1969) *Biochemistry* **8,** 435–443
24. Rajagopalan, P. T. R., Datta, A., and Pei, D. (1997) *Biochemistry* **36,** 13910–13918